

Self-doping induced orbital-selective Mott transition in $\text{Hg}_2\text{Ru}_2\text{O}_7$

L. Craco,^{1,2} M. S. Laad,² S. Leoni,¹ and H. Rosner¹¹Max-Planck-Institut für Chemische Physik fester Stoffe, 01187 Dresden, Germany²Max-Planck-Institut für Physik komplexer Systeme, 01187 Dresden, Germany

(Received 15 December 2008; published 26 February 2009)

Pyrochlore oxides are fascinating systems where strong multiorbital correlations in concert with geometrical frustration give rise to unanticipated physical properties. The detailed mechanism of the insulator-metal transitions (IMTs) underpinning these phenomena is, however, ill understood in general. Motivated thereby, we study the IMT in the pyrochlore $\text{Hg}_2\text{Ru}_2\text{O}_7$ using local-density approximation plus dynamical mean-field theory. In contrast to the well-known examples of Mott transitions in transition metal oxide, we show that in the negative charge-transfer situation characteristic of $\text{Hg}_2\text{Ru}_2\text{O}_7$, self-doping plays a crucial role in the emergence of an orbital-selective IMT. We argue that this mechanism has broader relevance to other correlated pyrochlore oxides.

DOI: 10.1103/PhysRevB.79.075125

PACS number(s): 71.28.+d, 71.30.+h, 72.10.-d

I. INTRODUCTION

The Mott-Hubbard insulator-metal transition (IMT) is by now recognized to play a central role in our understanding of d - and f -band compounds.¹ Understanding the complex interplay between strong multiorbital (MO) electronic correlations, structural distortions, and strongly anisotropic orbital-dependent hopping holds the key to a consistent theoretical description of their unique responses. Adding geometric frustration to the above results in a truly formidable problem. In geometrically frustrated systems, the exponentially large degeneracy of classical ordered states inhibits emergence of conventional order, permitting new, complex ordered ground states to arise.² In *real* systems, structural effects may partially remove this huge degeneracy, making the problem (counterintuitively) somewhat simpler to solve.³ However, in near-undistorted cases, near-perfect orbital degeneracy, and the consequent strong quantum orbital *and* spin fluctuations in a highly degenerate system underpin their physical behavior.

The recently discovered pyrochlore system, $\text{Hg}_2\text{Ru}_2\text{O}_7$,⁴ is a particularly interesting case in this context. As temperature (T) is reduced, the anomalous (see below) non-Fermi-liquid (nFL) metallic state becomes unstable, via a first-order Mott transition, to an antiferromagnetic (AF) Mott-Hubbard insulator (AFI).⁵ External pressure (p) melts the AFI beyond a critical $p_c=6.0$ GPa, resulting in a low- T correlated FL behavior for $T < T^*=13$ K. At ambient pressure, the IMT transition is accompanied by lowering of lattice symmetry from (high- T) cubic to a (low- T) lower, hitherto precisely unknown, type: depending upon its precise type, either AF or dimer order may be possible.⁶

The high- $T > T^*$ state in $\text{Hg}_2\text{Ru}_2\text{O}_7$ is an anomalous nFL: the dc resistivity $\rho(T) \approx T$ for $T > T_{\text{MI}}=108$ K (Ref. 4) at ambient pressure, and deviates from the FL form for $T > T^*$ beyond p_c . The uniform spin susceptibility is Curie-Weiss type for $T > T_{\text{MI}}$, indicating a strong local-moment scattering regime. The nFL character is also borne out from the recent photoemission (PES) data,⁷ showing anomalously broad PES line shapes, with no hint of Fermi-liquid (FL) quasiparticles, in the metallic phase. Given the cubic pyrochlore structure

for $T > T_{\text{MI}}$, strong orbital (from t_{2g} orbital degeneracy) and spin fluctuations are implied. How might strong scattering processes involving these fluctuations produce the observed nFL metal? What drives the AFI as T is lowered? A correlated electronic structure study which can illuminate these issues does not, to our best knowledge, exist. In this work we study precisely these issues in part in $\text{Hg}_2\text{Ru}_2\text{O}_7$ using the local-density approximation plus dynamical mean-field theory (LDA+DMFT) method.⁸ We focus on the mechanism of the T -driven IM transition, and leave the issue of the low-dimensional AF with a spin gap for future consideration.

II. MODEL AND SOLUTION

Starting with the high- T cubic $Fd\bar{3}m$ structure found by Klein *et al.*,⁴ LDA band-structure calculations were performed using a (scalar and fully relativistic) full-potential local-orbital (FPLO) scheme⁹ and a linear muffin-tin orbital (LMTO) scheme in the atomic sphere approximation.¹⁰ In Fig. 1 we display our FPLO-LDA (Ref. 11) results for the one-particle density of states (DOS). Clearly, the major contribution to the DOS comes from Ru $4d$ and O(1) $2p$ orbitals, but the O(2) $2p$ orbitals also have noticeable spectral weight at the Fermi level (E_F). As seen in Fig. 1, the influence of the spin-orbit coupling in the cubic phase to the t_{2g} states near E_F is negligible. Further, we observe strong hybridization between Ru $4d$ -O(1) $2p$ orbitals, and between O(2) $2p$ -Hg $6s$ orbitals, but weak mixing between these two sets. These important findings will be exploited below to study the physics of $\text{Hg}_2\text{Ru}_2\text{O}_7$ using a multiorbital Hubbard model involving only the d -band sector. At one-particle level, the corresponding model Hamiltonian reads $H_{\text{band}} = \sum_{k,a,\sigma} \epsilon_{ka} d_{k\sigma}^\dagger d_{k\sigma} + \sum_{i,a,b=1,2} \Delta_b (n_{i,b}^p - n_{i,a}^d)$, where a labels the diagonalized combination of $(e'_{g1}, e'_{g2}, a'_{1g})$ (Ref. 12) the t_{2g} orbitals, Δ_b ($b=1,2$) are the pd charge-transfer (CT) terms involving two Ru-O(1) ($b=1$) and Ru-O(2) ($b=2$) channels. Clearly, neither an AFI nor a nFL metal can be expected at this level, this requiring a reliable treatment of strong d -shell electronic correlations. This part reads

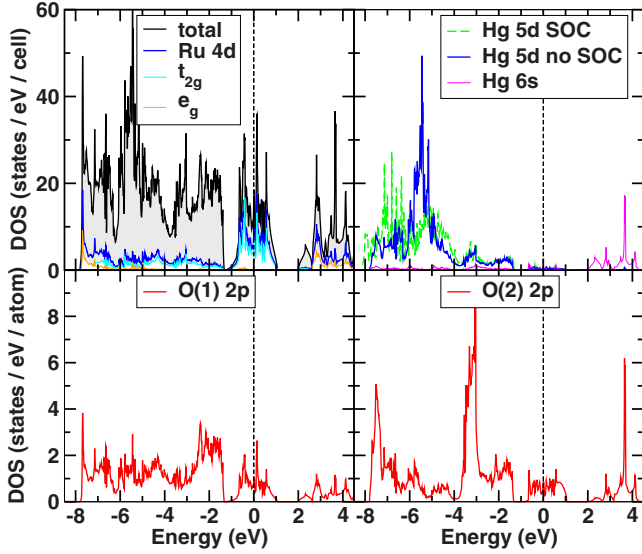


FIG. 1. (Color online) LDA band structure for cubic $\text{Hg}_2\text{Ru}_2\text{O}_7$. O(1) [O(2)] denotes oxygen ions nearest to Ru (Hg).

$$H_{\text{int}} = U \sum_{i,a} n_{ia\uparrow}^d n_{ia\downarrow}^d + U' \sum_{i,a,a'} n_{ia}^d n_{ia'}^d - J_H \sum_{i,a,a'} \mathbf{S}_{ia} \cdot \mathbf{S}_{ia'}, \quad (1)$$

with $a, a' = e'_{g1}, e'_{g2}, a_{1g}$. Given the larger spatial extent of $4d$ orbital vis-à-vis their $3d$ counterpart, we also include a Madelung term, $H_M = U_{pd} \sum_{(i,j),a,b} n_{ia}^d n_{jb}^p$, in our calculations (see below). In $\text{Ti}_2\text{Mn}_2\text{O}_7$, the IMT [from a paramagnetic insulator (PI) to a ferromagnetic metal (FMM)] is seemingly driven by the $\text{Ti } 6s$ states crossing E_F across T_c ,¹³ for instance. This can occur via a T -dependent CT from the TM d states to the O(2)-Ti hybridized states. In view of the generic relevance of *self-doping* in TM $4d$ pyrochlores,^{13,14} this term is an essential part. In the low- T phase, this will involve CT processes involving the O $2p$ -Hg $6s$ channel (second term of H_{band}) across the IMT, as we describe below.

The $d_{a\sigma}$ above should be understood as appropriate RuO_6 cell-centered combinations of the Ru $4d$ and O $2p$ orbitals, computed within LDA. Similarly, the $b=2$ channel is to be understood as a band of hybridized O $2p$ and Hg $6s$ orbital states. Because of the negligible one-particle mixing (hybridization) between the $b=1,2$ channels, we approximate the full problem of three Ru d bands coupled to the $b=2$ band channel by replacing the latter by a “reservoir,” whose only function is to simulate the self-doping process arising from the negative charge-transfer situation that is obtained in $\text{Hg}_2\text{Ru}_2\text{O}_7$. Of course, this is an approximation. It is, however, a good one: the $b=2$ band channel has appreciably smaller DOS around E_F in the LDA results. In a DMFT-like approximation, with negligible one-particle hybridization between the $b=1,2$ bands, the *intersite* Madelung term will push this small spectral weight away from E_F , to lower and higher energies. (Notice that the O $2p$ bands will be split by $U_{pd}z\langle n_d \rangle$, where z is the coordination number of the lattice, and hence quite large.) This will already occur at the level of LDA+Hartree approximation. We then expect that the *correlated* spectral function will be dominated by the d bands over an appreciable range about E_F . Correlation effects in

$\text{Hg}_2\text{Ru}_2\text{O}_7$ via LDA+DMFT are studied below, subject to this caveat. We will show that this is indeed a good approximation *a posteriori*, in the sense that our LDA+DMFT results with the above caveat show very good quantitative agreement with one-particle spectroscopy and key thermodynamic and transport data in $\text{Hg}_2\text{Ru}_2\text{O}_7$.

The full many-body Hamiltonian reads $H = H_{\text{band}} + H_{\text{int}} + H_M$. We solve this model within MO-DMFT developed and used for a range of transition metal oxide (TMO) with good success.⁸ We use the MO-iterated perturbation theory (IPT) as an impurity solver in the DMFT self-consistent procedure. Though not numerically exact [such as quantum Monte Carlo (QMC), numerical renormalization group (NRG), and dynamic density matrix renormalization group (D-DMRG)], it has many advantages: it is valid for $T=0$, where QMC cannot be used. NRG and D-DMRG are extremely prohibitive for three orbital models, even without electronic structural inputs at LDA level. As shown in earlier work,¹⁵ DMFT(MO-IPT) generically gives very good semiquantitative agreement with PES and x-ray-absorption (XAS) experiments for TMOs.^{15,16} For $\text{Hg}_2\text{Ru}_2\text{O}_7$, DMFT(MO-IPT) has to be extended to treat the second CT channel described above. Given the complexity of the problem, we choose the following strategy to solve H above. For the high- T phase, (i) we solve $H_{\text{band}} + H_{\text{int}}$ within DMFT(MO-IPT) version used earlier; for technical details see Ref. 15. (ii) As indicated by experiment on the related $\text{Ti}_2\text{Ru}_2\text{O}_7$ system,¹⁴ we study the effect of Ru $4d$ -O(2) $2p$ -Hg $6s$ CT processes by incorporating this CT channel self-consistently into the LDA+DMFT(MO-IPT) procedure: given the small Ru $4d$ -O(2) $2p$ hybridization, the O(2) $2p$ -Hg $6s$ channel acts like a *scattering* (nonhybridizing) channel for the Ru t_{2g} bands in the impurity model of MO-DMFT. This enables us to treat this extra channel by combining the MO-IPT solution for (i) with the *exact* DMFT solution of a Falicov-Kimball model (FKM) for (ii),¹⁷ in a self-consistent way.

III. LDA+DMFT RESULTS AND DISCUSSION

We now describe our LDA+DMFT results. We start with the (cubic) pyrochlore structure at high T , with the corresponding LDA DOS as the input for the MO-DMFT calculation with total $4d$ occupation, $n_f=3$. Further, we work in the LMTO (Ref. 18) representation in which the one-particle density matrix is diagonal in the t_{2g} orbital index, so that $G_{\alpha\beta}^{(0)}(k, \omega) = \delta_{\alpha\beta} G_{\alpha\alpha}^{(0)}(k, \omega)$. We choose $U=5.5$ eV, $J_H=1.0$ eV, and $U' \approx (U-2J_H)=3.5$ eV for the Ru $4d$ shell, along with $U_{pd} \approx 1.5$ eV, as representative values for $\text{Hg}_2\text{Ru}_2\text{O}_7$. We believe that U, J_H do not vary much for $4d$ TMO pyrochlores and, in fact, $U=5.0$ eV was found for the CT insulator Cs_2AgF_4 .¹⁹

A. Metallic phase

In Fig. 2, we show the correlated many-particle spectral function for the metallic phase of $\text{Hg}_2\text{Ru}_2\text{O}_7$. The dynamical spectral weight transfer (SWT) over large energy scales, characteristic of strong local correlations, is explicitly manifest. More interestingly, the metal has an orbital-selective

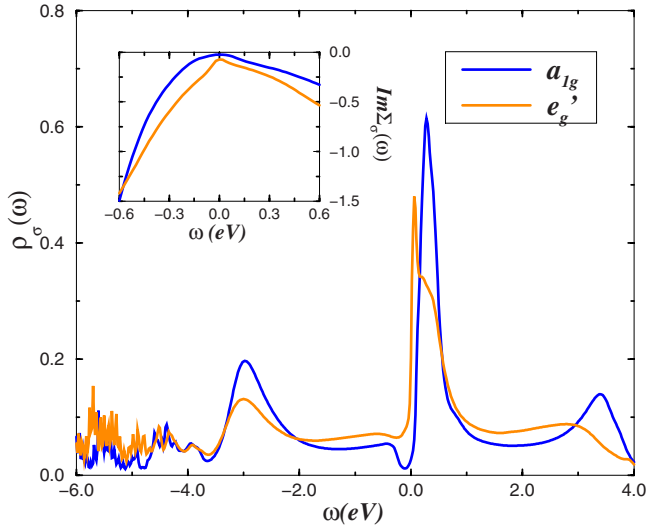


FIG. 2. (Color online) t_{2g} -resolved LDA+DMFT densities of states for $\text{Hg}_2\text{Ru}_2\text{O}_7$ in the high- T nFL phase, for $U=5.5$ eV and $J_H=1$ eV. Notice the orbital-selective (OS) nature of the metal, as well as the nFL character in the orbital-resolved self-energies (see inset).

(OS) character: the a_{1g} DOS is almost ‘‘Mott’’ localized, even as the e'_g DOS develops a precursor of a low-energy pseudogap, characteristic of an incoherent metal behavior. This is further corroborated by examining the orbital-dependent self-energies $[\Sigma(\omega)]$; see inset of Fig. 2. Clearly, the e'_g (imaginary part of) $\Sigma(\omega)$ shows *quasilinear* frequency dependence near the Fermi energy ($|\omega - E_F| < 0.3$ eV), while $\text{Im} \Sigma_{a_{1g}}(\omega)$ shows quadratic behavior. This describes a nFL metal, with a linear-in- T quasiparticle damping rate. Within DMFT, this is also the transport relaxation rate,²⁰ since vertex corrections drop out in the computation of the conductivities in this limit. The dc resistivity is then given by $\rho_{\text{dc}}(T) \approx (m^*/ne^2)\text{Im} \Sigma_{e'_g}(\omega=T) \approx AT$, in accord with the linear-in- T resistivity observed experimentally in the ‘‘high- T ’’ metallic phase. Moreover, the selective localization seen in the a_{1g} orbital DOS gives rise to unquenched local moments coexisting with ‘‘itinerant’’ (but incoherent as derived above) e'_g carriers naturally gives a Curie-Weiss form of the spin susceptibility, which is also observed right up to the IMT. We have also estimated the γ coefficient of the metallic specific heat from the real part of $\Sigma_\alpha(\omega)$ (not shown) as $\gamma/\gamma_{\text{LDA}}=4.25$: this seems to be in the range estimated in Ref. 4. Actually, the noticeable T dependence of γ above T_{MI} (Ref. 4) is additional evidence of disordered local moments in the ‘‘bad’’ metal, and further supports our picture.

Using the LDA+DMFT result, we also compare (Fig. 3) our computed PES line shape with very recent work from the RIKEN-SPring 8 group.⁷ Given our restriction to the t_{2g} -Ru $4d$ bands in the MO-DMFT (Hg d and O $2p$ bands will start contributing at higher binding energies, as seen from LDA), good quantitative agreement with experiment is evident up to -2.0 eV, lending strong support to our theoretical work. Additionally, we predict that an intense peak will be seen around 0.4–0.5 eV in x-ray absorption studies, as in $\text{Ti}_2\text{Ru}_2\text{O}_7$.²¹

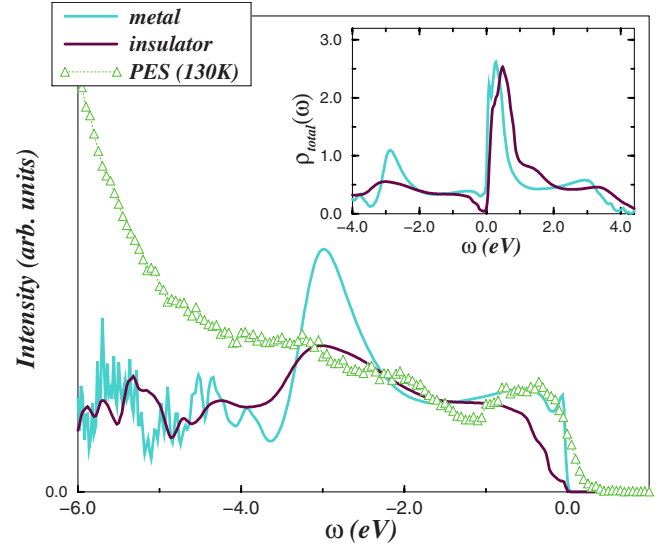


FIG. 3. (Color online) Theoretical PES spectra (LDA+DMFT DOS convoluted with instrumental resolution) in the nFL metallic and insulating phases of $\text{Hg}_2\text{Ru}_2\text{O}_7$. In the LDA+DMFT calculation, the total t_{2g} electron density changes from $\langle n_t \rangle = 3.0$ (metallic) to $\langle n_t \rangle = 2.6$ (insulating). The theoretical result shows very good agreement with experimental PES result in the metallic phase, taken from Ref. 7, up to 2 eV binding energy. The inset shows the total spectral function.

In fact, the LDA+DMFT spectral functions show that at low energy the full MO problem is mapped onto an effective FKM-like model,¹⁵ since the bad metal is of the orbital-selective type. There, the problem in the local limit corresponds to itinerant (but incoherent) e'_g carriers scattering off (Mott) localized a_{1g} electronic states. The resulting problem is precisely the ‘‘x-ray-edge’’ problem in DMFT.²² We now understand the structure of the self-energies, and the nFL behavior, as an interesting manifestation of the Anderson orthogonality catastrophe (OC) caused by this x-ray-edge mapping. Building upon this understanding, using DMFT, we predict for $T > T_{\text{MI}}$ the following:

(a) The optical conductivity will show a low-energy pseudogapped form, characteristic of an incoherent (nFL) metal. Polarized optical studies should indicate the OS character of the nFL state.

(b) Given the local version of the Shastry-Shraiman relation,²³ the electronic Raman line shape should show a continuum response, cut off by a pseudogap feature at low energy.

B. Insulating phase

Now, we turn to a description of the insulating phase. A naive search for the instability of the nFL to a Mott-Hubbard insulating state, where U, U' were increased to unphysical values, nevertheless turned out to be unsuccessful. This is a clear indication of involvement of additional electronic-cum-structural effects in driving the IMT. The observed structural change across T_{MI} (Refs. 4 and 5) supports this reasoning. From the LDA orbital assignment, it is clear that an additional structural change necessarily involves *partial* occupa-

tion of the twofold-degenerate e'_g orbitals. Starting from the nFL metal derived above, this can only occur via a T -dependent change in the “self-doping” process.¹⁴ As in $\text{Ti}_2\text{Ru}_2\text{O}_7$, this T dependence could be provided by electronic coupling to the Ru-O stretching phonon mode, which is experimentally observed to split below T_{MI} .¹⁴ This would imply a structural change setting in below T_{MI} , whose precise nature is hitherto unknown.

Motivated by this observation, we argue that this resulting change in the Ru $4d \rightarrow \text{O}(2) 2p$ CT leads to a partial $4d$ occupation, induces orbital order, and lifts the e'_g degeneracy via a structural distortion. Within DMFT, this will reduce the orbital-dependent hoppings, driving large SWT from low to high energy, and stabilize the second (Mott-Hubbard insulating) solution of the DMFT equations. This is indeed seen in the LDA+DMFT calculation, as we show below.

Based on this reasoning, we explore the Mott-Hubbard insulating phase of $\text{Hg}_2\text{Ru}_2\text{O}_7$ by searching numerically for the instability of the first (metallic) solution found above to the second (insulating) solution of the DMFT equations in the quantum paramagnetic phase. The DMFT(MO-IPT) equations are solved with U , U' , U_{pd} , and $n_f=2.6$. We vary n_t in trial steps, and look for a critical $n_t^{(c)}$ which stabilizes the PI solution of the DMFT equations. As discussed above, and indeed seen in the inset of Fig. 3, partial occupation of the $4d-e'_g$ orbitals leads to removal of the orbital degeneracy, and the corresponding modification of orbital orientation gives rise to a reduced *intersite* one-electron overlap. Within MO-DMFT, this triggers the Mott-Hubbard insulating state via large SWT on a scale of 5.0 eV, as seen in Fig. 2. Hence, the IMT is an OS Mott transition. Importantly, however, notice that the self-doping process leading to fractional d -orbital occupation is a crucial ingredient. Thus, in contrast to other OS cases,¹⁵ the IMT in $\text{Hg}_2\text{Ru}_2\text{O}_7$ is driven by the self-doping in the negative CT situation, $\Delta_2=(\epsilon_{p2}-\epsilon_d) = (-2.8 \text{ eV} + 1.3 \text{ eV}) = -1.5 \text{ eV}$. Along with the microscopic elucidation of the nFL behavior, the agreement with PES in the nFL metal phase up to $\omega \approx -2.0 \text{ eV}$ (Fig. 3) constitutes strong evidence in favor of our mechanism for the IMT in $\text{Hg}_2\text{Ru}_2\text{O}_7$. Quantitative comparison with PES in the low- T phase requires an extension of our approach to include short-ranged (*intersite*) orbital and spin correlations characteristic of pyrochlores. This requires a cluster-DMFT analysis, presently a forbidding prospect. Nevertheless, observation of a Curie-Weiss spin susceptibility right up to the IMT,^{6,24} along with the excellent agreement with PES in the nFL, justifies the use of DMFT to describe the IMT.

We emphasize that this is a different picture for the IMT in correlated systems. In contrast to the early TMO, which are Mott-Hubbard insulators ($U_{dd} > \Delta$ in the Zaanen-Sawatzky-Allen scheme),²⁵ the Ru $4d\text{-O}(1) 2p$ CT channel, along with the Madelung term, is important in $\text{Hg}_2\text{Ru}_2\text{O}_7$. In the DMFT context, the importance of the CT energy in the late-TMO is recognized.²⁶ Our work shows the relevance of CT energy for the IMT in a MO pyrochlore system. Further, it is likely to be more broadly generic to pyrochlore TMOs. Recall that in $\text{Ti}_2\text{Mn}_2\text{O}_7$, the PI-FMM (Ref. 13) transition is driven by the shift of the Ti $6s$ band through E_F across T_c . This is readily rationalized in our picture, in terms of the “switching on” of the Mn $3d\text{-O}(2) 2p\text{-Ti } 6s$ CT channel across T_c in $\text{Ti}_2\text{Mn}_2\text{O}_7$.¹³

The correlation between the CT process detailed above and the IMT is also visible in a whole family of $4d$ pyrochlores, $A_2\text{Ru}_2\text{O}_7$, with $A=\text{Pb,Bi,Y}$.²¹ The low- T magnetic ordering in the Mott-Hubbard insulating phase(s) may, however, be quite different, being sensitively dependent on the nature of the structural change across the IMT, as well as on spin state. For example, the spin $S=1$ system, $\text{Ti}_2\text{Ru}_2\text{O}_7$, shows a very similar Mott transition; however, the low- T phase is found to be a Haldane spin chain.²⁷ In $\text{Hg}_2\text{Ru}_2\text{O}_7$, the half-integer spin $S=3/2$ rules out the Haldane analogy. If the low- T magnetic structure corresponds to having Ru chains, as in $\text{Ti}_2\text{Ru}_2\text{O}_7$, one would have an AF ground state with gapless spin excitations. Observation of the spin gap in the uniform spin susceptibility in $\text{Hg}_2\text{Ru}_2\text{O}_7$ may therefore point to the relevance of the spin-orbit coupling in the *insulating* phase: this will induce Ising-type anisotropy in an $S=3/2$ Heisenberg chain and generate a gap to spin excitations.²⁸ More experimental work is also called for to pinpoint the specific factors affecting this issue. Given the structural distortion necessarily accompanying the IMT caused by lifting of the e'_g degeneracy in $\text{Hg}_2\text{Ru}_2\text{O}_7$, more detailed theoretical work awaits more precise characterization of the low- T structure of $\text{Hg}_2\text{Ru}_2\text{O}_7$. We plan to address the issue of magnetic order and its associated excitation spectrum in the low- T (insulating) phase of $\text{Hg}_2\text{Ru}_2\text{O}_7$ in a future work.

IV. CONCLUSION

In conclusion, we have performed LDA+DMFT calculations to demonstrate the role of multiorbital electron-electron interactions on the electronic structure of a recently discovered pyrochlore system, $\text{Hg}_2\text{Ru}_2\text{O}_7$. This system exhibits a first-order temperature-dependent IMT. The high- T metallic phase is shown to be an orbital-selective non-Fermi liquid, signaled by a quasilinear frequency dependence of the imaginary part of the correlated self-energy and the absence of quasiparticle peaks in the orbital-selective spectral functions at very low frequencies. The LDA+DMFT spectral function shows good quantitative agreement with recent PES data, showing anomalously broad PES line shapes, as well as with the linear-in- T resistivity and mass enhancement in the metallic phase. In stark contrast to the better-known examples¹ of Mott transitions in $3d$ transition-metal compounds, our results imply a different mechanism for MIT in the $4d$ pyrochlore-based electron systems (such as $\text{Hg}_2\text{Ru}_2\text{O}_7$). Namely, a negative charge-transfer associated self-doping drives an orbital-selective MIT at low temperatures via the Mott-Hubbard route. Our study should be more generally applicable to MO pyrochlore systems and, in particular, to $\text{Ti}_2\text{Mn}_2\text{O}_7$, exhibiting Mott-Hubbard transitions^{14,21,24,29} as functions of suitable “tuning parameters.”

ACKNOWLEDGMENTS

We are indebted to A. Chainani for discussions and, especially, for sending us his unpublished PES results. L.C. and H.R. thank the Emmy-Noether Program of the DFG for support.

- ¹M. Imada, A. Fujimori, and Y. Tokura, *Rev. Mod. Phys.* **70**, 1039 (1998).
- ²K. S. Raman, R. Moessner, and S. L. Sondhi, *Phys. Rev. B* **72**, 064413 (2005), and references therein.
- ³S. Di Matteo, G. Jackeli, C. Lacroix, and N. B. Perkins, *Phys. Rev. Lett.* **93**, 077208 (2004).
- ⁴W. Klein, R. K. Kremer, and M. Jansen, *J. Mater. Chem.* **17**, 1356 (2007).
- ⁵A. Yamamoto, P. A. Sharma, Y. Okamoto, A. Nakao, H. A. Katori, S. Niitaka, D. Hashizume, and H. Takagi, *J. Phys. Soc. Jpn.* **76**, 043703 (2007).
- ⁶N. Takeshita, C. Terakura, Y. Tokura, A. Yamamoto, and Hide-nori Takagi, *J. Phys. Soc. Jpn.* **76**, 063707 (2007).
- ⁷A. Chainani (private communication).
- ⁸G. Kotliar, S. Y. Savrasov, K. Haule, V. S. Oudovenko, O. Parcollet, and C. A. Marianetti, *Rev. Mod. Phys.* **78**, 865 (2006); K. Held, *Adv. Phys.* **56**, 829 (2007).
- ⁹K. Koepnik and H. Eschrig, *Phys. Rev. B* **59**, 1743 (1999).
- ¹⁰O. K. Andersen, *Phys. Rev. B* **12**, 3060 (1975).
- ¹¹Self-consistency was obtained on a $12 \times 12 \times 12$ k mesh for the full Brillouin zone.
- ¹²Within the LMTO framework, the diagonalized combination of the t_{2g} orbitals reads $|e'_{g1}\rangle \approx 0.195(|d_{xz}\rangle - |d_{yz}\rangle) + 0.888|d_{x^2-y^2}\rangle$, $|e'_{g2}\rangle \approx 0.888|d_{z^2}\rangle + 0.112(2|d_{xy}\rangle + |d_{yz}\rangle + |d_{zx}\rangle)$, $|a_{1g}\rangle = 0.577(|d_{yz}\rangle + |d_{zx}\rangle - |d_{xy}\rangle)$.
- ¹³A. P. Ramirez and M. A. Subramanian, *Science* **277**, 546 (1997).
- ¹⁴J. S. Lee, Y. S. Lee, K. W. Kim, T. W. Noh, J. Yu, T. Takeda, and R. Kanno, *Phys. Rev. B* **64**, 165108 (2001).
- ¹⁵M. S. Laad, L. Craco, and E. Müller-Hartmann, *Phys. Rev. B* **73**, 045109 (2006).
- ¹⁶O. Miura and T. Fujiwara, *Phys. Rev. B* **77**, 195124 (2008).
- ¹⁷Q. Si, G. Kotliar, and A. Georges, *Phys. Rev. B* **46**, 1261 (1992).
- ¹⁸Self-consistency is reached by performing calculations on a $12 \times 12 \times 12$ k mesh for the Brillouin integration. The radii of the atomic spheres were chosen as $r=2.8781$ (Hg), $r=1.8712$ and 2.1247 [O(1) and O(2)], and $r=2.4971$ (Ru) (in a.u.) in order to minimize their overlap.
- ¹⁹D. Kasinathan, K. Koepnik, U. Nitzsche, and H. Rosner, *Phys. Rev. Lett.* **99**, 247210 (2007).
- ²⁰A. Georges, G. Kotliar, W. Krauth, and M. J. Rozenberg, *Rev. Mod. Phys.* **68**, 13 (1996).
- ²¹J. Okamoto, T. Mizokawa, A. Fujimori, T. Takeda, R. Kanno, F. Ishii, and T. Oguchi, *Phys. Rev. B* **69**, 035115 (2004).
- ²²P. W. Anderson, *Phys. Rev. Lett.* **18**, 1049 (1967).
- ²³B. S. Shastry and B. I. Shraiman, *Phys. Rev. Lett.* **65**, 1068 (1990).
- ²⁴J. Okamoto, S.-I. Fujimori, T. Okane, A. Fujimori, M. Abbate, S. Yoshii, and M. Sato, *Phys. Rev. B* **73**, 035127 (2006).
- ²⁵J. Zaanen, G. A. Sawatzky, and J. W. Allen, *Phys. Rev. Lett.* **55**, 418 (1985).
- ²⁶J. Kunes, V. I. Anisimov, S. L. Skornyakov, A. V. Lukoyanov, and D. Vollhardt, *Phys. Rev. Lett.* **99**, 156404 (2007).
- ²⁷S. Lee, J.-G. Park, D. T. Adroja, D. Khomskii, S. Streltsov, K. A. McEwen, H. Sakai, K. Yoshimura, V. I. Anisimov, D. Mori, R. Kanno, and R. Ibberson, *Nature Mater.* **5**, 471 (2006).
- ²⁸I. Affleck, in *Fields, Strings and Critical Phenomena*, Proceedings of the Les Houches Summer School, Les Houches, France, 1988, edited by E. Brézin and J. Z. Justin (Elsevier, Amsterdam, 1989), Vol. 49.
- ²⁹J. S. Lee, S. J. Moon, T. W. Noh, T. Takeda, R. Kanno, S. Yoshii, and M. Sato, *Phys. Rev. B* **72**, 035124 (2005); A. Higashiya, S. Imada, A. Yamasaki, A. Irizawa, A. Sekiyama, S. Suga, Y. Taguchi, M. Iwama, K. Ohgushi, and Y. Tokura, *ibid.* **75**, 155106 (2007); R. S. Singh, V. R. R. Medicherla, K. Maiti, and E. V. Sampathkumaran, *ibid.* **77**, 201102(R) (2008).